Chapter 4

Yield and Ultimate Tensile Strength Models

The conventional method for developing a new weld metal with desired mechanical properties involves the design of a series of weld metals, varying chemical compositions and welding parameters. These welds are then manufactured and tested. A choice is then made of a particular combination of variables which best meets the requirements. Cost and time savings might be achieved with the help of appropriate models which reduce the number of steps needed.

The physical models discussed in Chapter 2, based on strengthening mechanisms, are not sufficiently sophisticated to enable a proper treatment of the problem. At the same time linear regression methods are not capable of representing the real behaviour which is far from linear when all the factors are taken into account.

On the other hand, the neural network method described in Chapter 3 is ideally suited to complex phenomena with many variables. In the present work, neural networks are used to model the yield strength and ultimate tensile strength of weld metal as a function of weld metal chemical composition, welding parameters and heat treatment conditions. Previous research along these lines by Cool *et al.* [27] was based on a rather limited database. The models are then used to design new alloys of use in the fabrication of power plant components.

4.1 Database

All of the data collected are from multirun weld deposits in which the joint is designed to minimise dilution from the base metal, to enable specifically the measurement of all–weld metal properties. Furthermore, they all represent electric arc welds made using one of the following processes: manual metal arc (MMAW), submerged arc welding (SAW) and tungsten inert gas (TIG). The welding process itself was represented only by the level of heat input. This is because a large number of published papers did not specify welding parameters in sufficient detail to enable the creation of a dataset without missing values. Missing values cannot be tolerated

in the method used here. If the effect of a welding process is not properly represented by the heat input and chemical composition, then neglect of any important parameters will make the predictions more 'noisy'. As discussed below, the noise in the output was found to be acceptable; a greater uncertainty arises from the lack of a uniform coverage of the input space. The data were collected from a large number of sources [28] to [88].

The aim of the neural network analysis was to predict the yield and tensile strength as a function of a large number of variables, including the chemical composition, the welding heat input and any heat treatment. The databases for the yield and ultimate tensile strength (UTS) are different because the UTS database also included the oxygen concentration since tensile failure should depend on inclusions which nucleate voids. As a consequence, the yield strength database consists of 2002 separate experiments whereas the UTS database is slightly smaller at 1972 experiments since the oxygen concentration was not always reported. Neural network method used in this work cannot cope with missing values of any of the variables. In 14 cases the sulphur and phosphorus concentrations were not available. Since these impurities might be important, it would not be satisfactory to set them to zero. Missing values of sulphur and phosphorus were therefore set at the average of the database.

4.1.1 Yield Strength Database

Table 4.1 shows the range, mean and standard deviation of each variable including the output (yield strength). The purpose here is simply to list the variables and provide an idea of the range covered. It is emphasised however, that unlike linear regression analysis, the information in Table 4.1 cannot be used to define the range of applicability of the neural network model. This is because the inputs are in general expected to interact. We shall see later that it is the Bayesian framework of our neural network analysis which allows the calculation of error bars which define the range of useful applicability of the trained network. A visual impression of the spread of data is shown in Fig. 4.1. It can be concluded from Fig. 4.1 that the effect on yield strength of carbon, manganese, silicon, nickel, molybdenum and heat input have been systematically studied. Hence, future experiments could focus on examining the effect of chromium in the range 3–8 wt%, vanadium (0.1–0.2 wt%), cobalt at all concentrations but in greater variety of alloy systems, tungsten at low and high concentrations, titanium and boron in high strength weld. The effect of tempering temperature in the range 250–500 °C also needs to be studied.

4.1.2 Ultimate Tensile Strength Database

Table 4.2 shows the range, mean and standard deviation of each variable including the output (ultimate tensile strength). The corresponding visual impression of the UTS database is similar

Input element	Minimum	Maximum	Mean	Standard deviation
Carbon (wt%)	0.01	0.22	0.072	0.025
Silicon (wt%)	0.01	1.63	0.344	0.138
Manganese (wt%)	0.27	2.31	1.192	0.41
Sulphur (wt%)	0.001	0.14	0.009	0.006
Phosphorus (wt%)	0.001	0.25	0.012	0.009
Nickel (wt%)	0.0	4.79	0.43	0.888
Chromium (wt%)	0.0	12.1	0.808	1.952
Molybdenum (wt%)	0.0	2.4	0.221	0.368
Vanadium (wt%)	0.0	0.32	0.026	0.06
Copper (wt%)	0.0	2.18	0.063	0.185
Cobalt (wt%)	0.0	2.8	0.007	0.115
Tungsten (wt%)	0.0	3.86	0.091	0.427
Titanium (p.p.m.)	0.0	900	64.9	112.14
Boron (p.p.m.)	0.0	195	5.8	19.08
Niobium (p.p.m.)	0.0	1770	69.6	168.13
Heat input (kJ mm^{-1})	0.55	7.9	1.6	1.234
Interpass temperature (°C)	20	375	207.8	52.67
Tempering temperature (°C)	20	780	358.3	249.29
Tempering time (h)	0.0	50	6.5	6.45
Yield strength (MPa)	288	1003	533.9	113.64

Table 4.1: The input variables for yield strength model. 'p.p.m.' corresponds to parts per million by weight.

to that of the yield strength. The UTS contains an extra input variable oxygen Fig. 4.2, the effect of which at higher concentrations (above 900 p.p.m.) needs to be studied.

4.2 Yield Strength Model

Some eighty yield strength neural network models were trained on a training dataset which consisted of a random selection of half the data (1001) from the yield strength dataset. The remaining 1001 data formed the test dataset which was used to see how the model generalises on unseen data. Each model contained the 19 inputs listed in Table 1 but with different numbers of hidden units or the random seeds used to initiate the values of the weights. Fig. 4.3 shows the results. As expected, the perceived level of noise (σ_ν) in the normalised yield strength decreases as the number of hidden units increases, Fig. 4.3a. This is not the case for the test error, which goes through a minimum at three hidden units, Fig. 4.3b, and for the log predictive error which reaches a maximum at six hidden units, Fig. 4.3c.

The error bars presented throughout this work represent a combination of the perceived level of noise σ_ν in the output and the fitting uncertainty estimated from the Bayesian framework. It

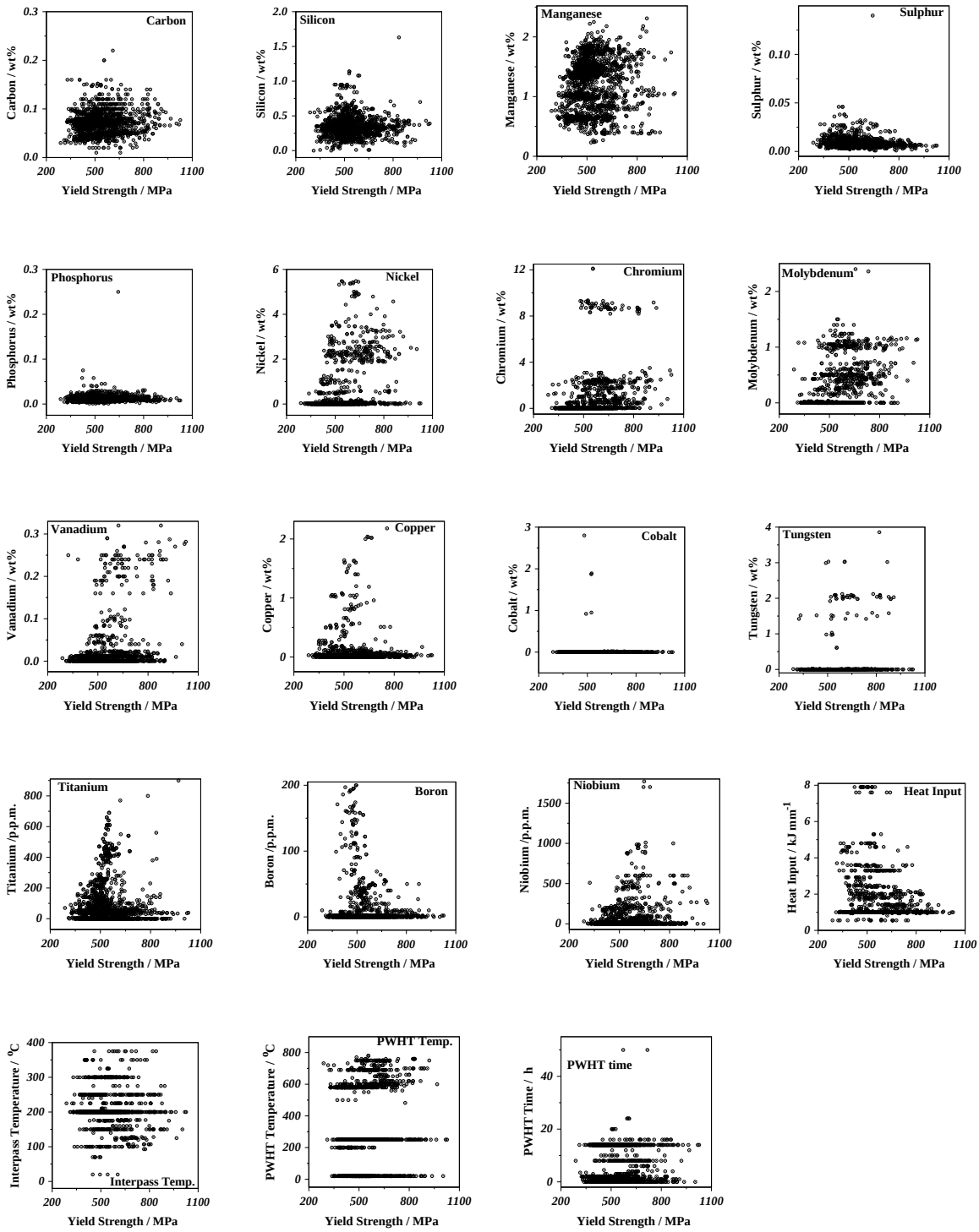

Figure 4.1: Database distribution used for yield strength model. 'p.p.m.' corresponds to parts per million by weight.

is evident that there are a few outliers in the plot of the predicted versus measured yield strength for the test dataset, Fig. 4.3f. Each of these outliers has been investigated and found to represent

Input element	Minimum	Maximum	Mean	Standard deviation
Carbon (wt%)	0.01	0.22	0.072	0.024
Silicon (wt%)	0.01	1.63	0.345	0.142
Manganese (wt%)	0.27	2.31	1.191	0.410
Sulphur (wt%)	0.001	0.14	0.009	0.006
Phosphorus (wt%)	0.001	0.25	0.012	0.009
Nickel (wt%)	0.0	4.79	0.426	0.900
Chromium (wt%)	0.0	12.1	0.748	1.810
Molybdenum (wt%)	0.0	2.4	0.219	0.370
Vanadium (wt%)	0.0	0.32	0.0252	0.060
Copper (wt%)	0.0	2.18	0.053	0.160
Cobalt (wt%)	0.0	2.8	0.008	0.110
Tungsten (wt%)	0.0	3.86	0.093	0.500
Oxygen (p.p.m.)	0.0	1650	362	200.8
Titanium (p.p.m.)	0.0	900	67	116.5
Boron (p.p.m.)	0.0	195	6	19.3
Niobium (p.p.m.)	0.0	1770	66	163.6
Heat input (kJ mm^{-1})	0.55	7.9	1.56	1.17
Interpass temperature (°C)	20	375	209	51.8
Tempering temperature (°C)	20	770	368	241.8
Tempering time (h)	0.0	50	6.9	6.5
Ultimate tensile strength (MPa)	440	1151	624	117.5

Table 4.2: The input variables for ultimate tensile strength model. 'p.p.m.' corresponds to parts per million by weight.

unique data which are not represented in the training dataset, Fig. 4.3e. For example, there is a weld with a sulphur concentration of 0.15 wt.% and another with a phosphorus concentration of 0.25 wt.%, both extremely high and unusual level of impurities in weld metals.

It is possible that a committee of models can make a more reliable prediction than an individual model (Chapter 3). The best models are ranked using the values of the log predictive errors Fig. 4.3c. Committees are then formed by combining the predictions of the best L models, where $L = 1, 2, \ldots$; the size of the committee is therefore given by the value of L. A plot of the test error of the committee versus its size gives a minimum which defines the optimum size of the committee, as shown in Fig. 4.3d.

The test error associated with the best single model is clearly greater than that of any of the committees Fig. 4.3d. The committee with twenty eight models was found to have an optimum membership with the smallest test error. The committee was therefore retrained on the entire data set without changing the complexity of any of its member models. The final comparison between the predicted and measured values of the yield strength for the committee of twenty eight is shown in Fig. 4.4.

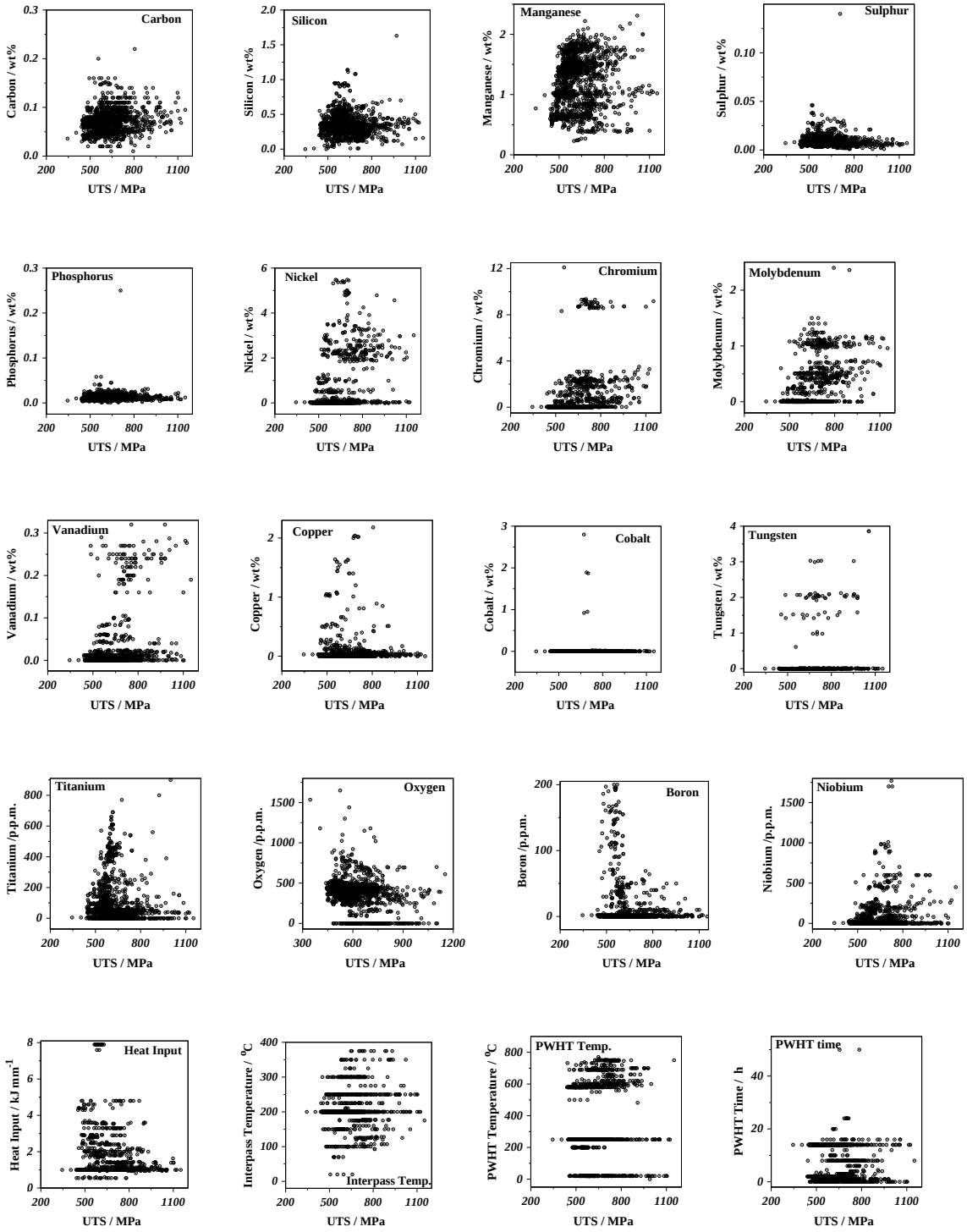

Figure 4.2: Database distribution used for ultimate tensile strength model. 'p.p.m.' corresponds to parts per million by weight.

Fig. 4.5 indicates the significance (σ_w) of each of the input variables, as perceived by first five neural network models in the committee. The σ_w value represents the extent to which a

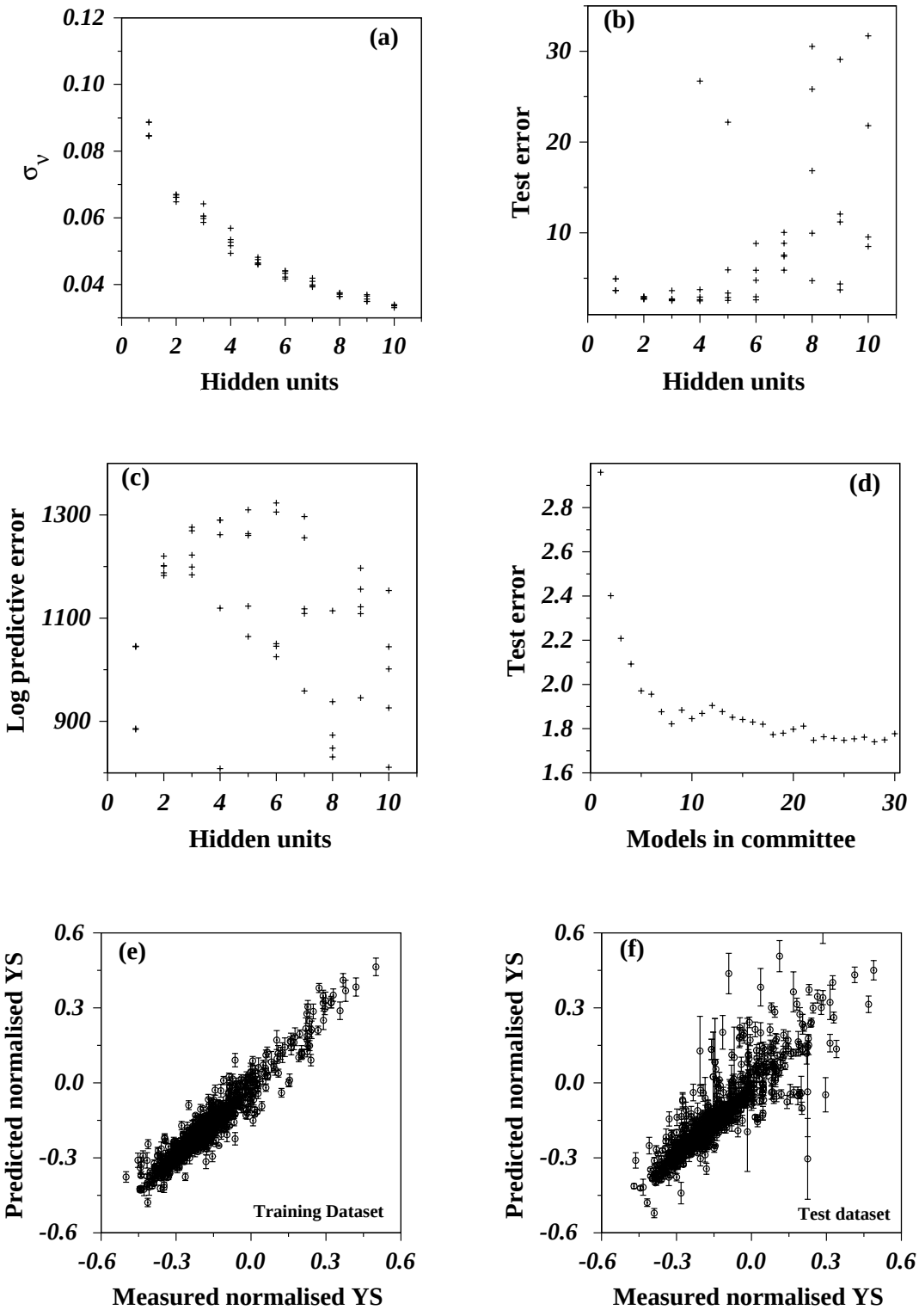

Figure 4.3: Yield strength (YS) model features.

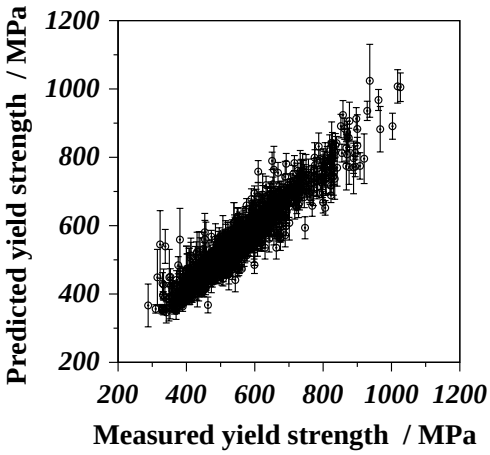

Figure 4.4: Yield strength model optimum committee model results.

particular input explains the variation in the output, rather like a partial correlation coefficient in linear regression analysis. The post-weld heat treatment temperature on the whole explains a large proportion of the variation in the yield strength Fig. 4.5. All of the variables considered are found to have a significant effect on the output indicating a good choice of inputs.

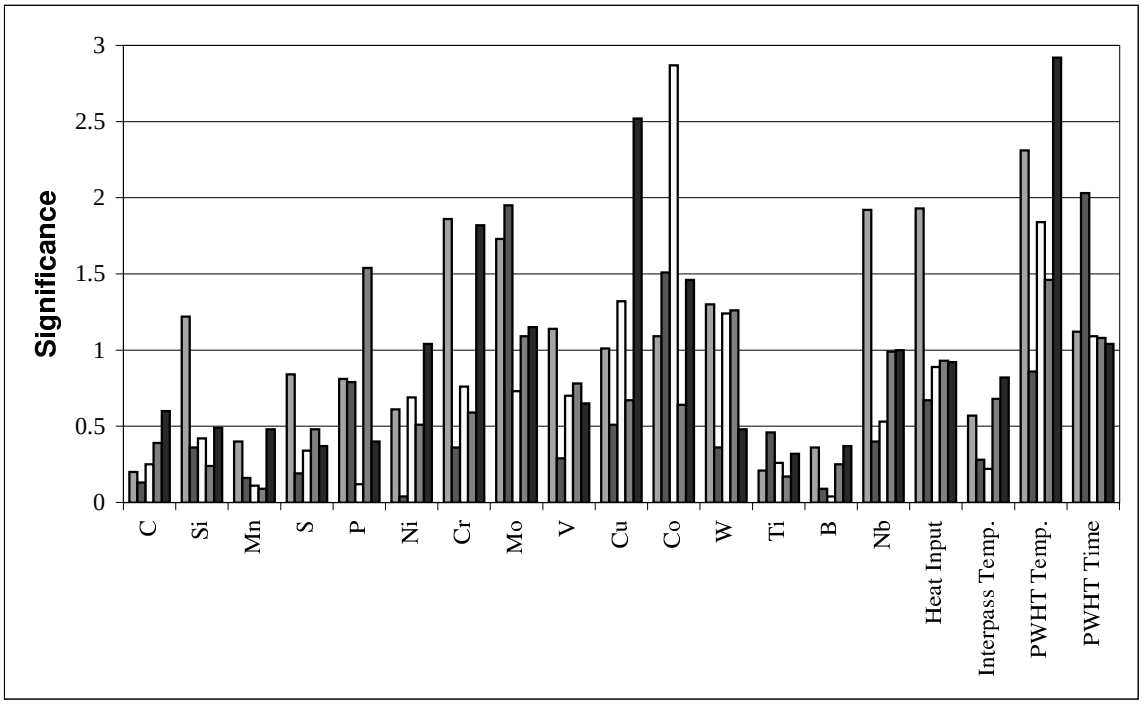

Figure 4.5: The perceived significance σ_w values of best five yield strength models for each of the inputs.

4.3 Ultimate Tensile Strength Model

The models were trained on 1972 individual experimental measurements, of which a random half of the data formed the training dataset and the other half the test dataset. The procedures are otherwise identical to those described for the yield strength model, resulting in the characteristics illustrated in Fig. 4.6 and the performance of the optimum committee of best models is illustrated in Fig. 4.7. The perceived significance values of the first five models are shown in Fig. 4.8. Here the additional input variable oxygen shows more significance along with post-weld heat treatment variables.

4.4 Application to C–Mn Weld Metals

Carbon–manganese weld metals refer to a popular class of ferritic steels in which the substitutional solutes other than silicon and manganese are generally kept to low concentration levels. They are interesting because there is a great deal already known about them, making it easy to interpret the physical significance of the neural network model. Furthermore, there exists an alternative semi–empirical model for the estimation of the yield and tensile strengths of such multirun welds [89] enabling a further comparison. The semi–empirical model is henceforth referred to as the "physical model" or PM for short. The basic values of the variables used in applying the model to carbon–manganese welds are listed in Table 4.3. The specified low–temperature heat treatment is simply a standard hydrogen removal treatment (250 °C for 14 h) applied to most welds before mechanical testing.

The results as a function of the carbon and manganese concentrations are illustrated in Fig. 4.9 for a variety of interesting cases. The calculated yield strength is in all cases found to be consistent with that expected from the physical model, although there are systematic differences at high yield strength values for all cases other than at the highest manganese concentration. However, the deviations are all within the error bounds of the neural network model for yield strength. The major discrepancies arise with the UTS especially at high UTS values. It is believed that the physical model is poorly constructed since the UTS is essentially taken arbitrarily to be linearly related to a single variable, the yield strength, Fig. 4.10 shows the comparison between the measured and strength estimation by the physical model. The physical model at higher strength values behaved very poorly; it estimated the strength higher than the measured.

An interesting feature of strengthening due to substitutional solutes is the synergistic effect with carbon. Fig. 4.11a and b shows that the dependence of the strengthening effect of molybdenum on the carbon concentration is particularly large; the effect of molybdenum in strengthening the weld is greater than that of Cr or Mn. This is consistent with published literature [90]. El-

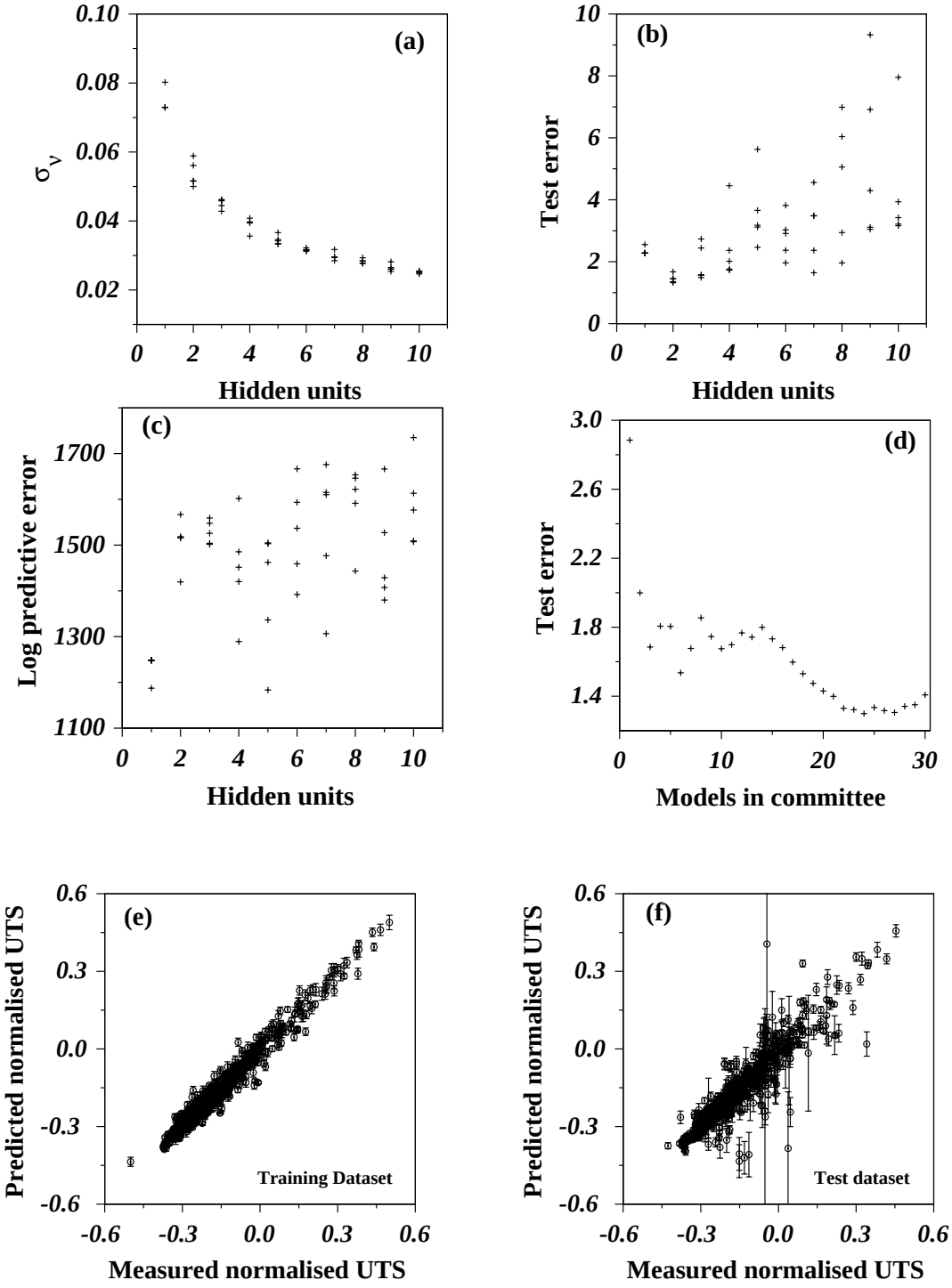

Figure 4.6: Ultimate tensile strength (UTS) model features.

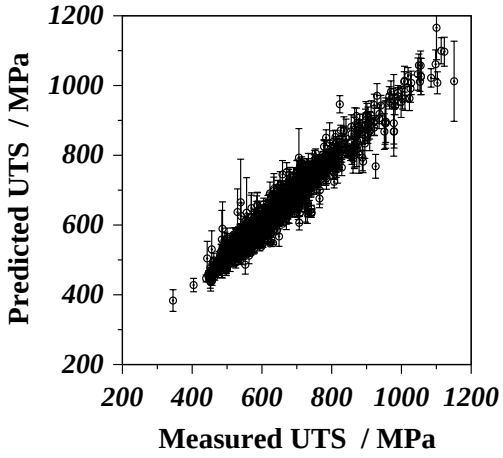

Figure 4.7: Ultimate tensile strength model optimum committee model results.

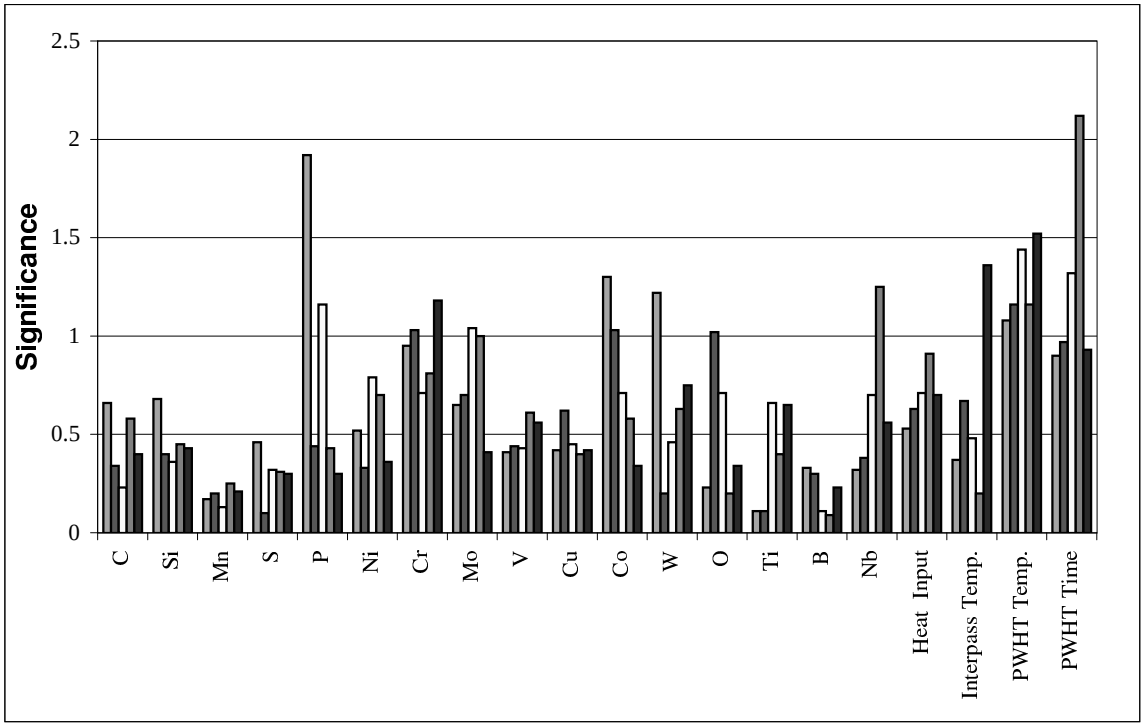

Figure 4.8: The perceived significance σ_w values of best five ultimate tensile strength models for each of the inputs.

ements such as molybdenum and vanadium are associated with strong secondary hardening effects which frequently trigger a reduction in toughness. In ordinary carbon–manganese multirun welds, the secondary microstructure, *i.e.* regions of weld metal which are tempered by subsequent weld runs, lose most of their microstructural strength. This is not necessarily the case in weld metal containing strong carbide formers. For example, it is well–established that

Input variable	
C (wt%)	0.06
Si (wt%)	0.5
Mn (wt%)	1.5
S (wt%)	0.006
P (wt%)	0.008
Ni (wt%)	0.0
Cr (wt%)	0.0
Mo (wt%)	0.0
V (wt%)	0.0
Cu (wt%)	0.0
Co (wt%)	0.0
W (wt%)	0.0
Ti (wt%)	0.0
O (p.p.m.)	300
B (p.p.m.)	0.0
Nb (p.p.m.)	0.0
Heat input (kJ mm^{-1})	1.14
Interpass temperature ($^{\circ}$C)	175
Tempering temperature ($^{\circ}$C)	250
Tempering time (h)	14

Table 4.3: The input variables of carbon–manganese steel weld metal used in the analysis.

the yield strength calculated using the Young–Bhadeshia model (Chapter 2) is always underestimated with molybdenum–containing welds, the degree of underestimation increasing with the molybdenum concentration [1]. The behaviour observed in Fig. 4.11a is not therefore surprising.

The sensitivity of strength to carbon concentration and the net magnitude of the strengthening effect decreases for the ultimate tensile strength, Fig. 4.11. This is expected since the UTS is measured at large plastic strains whereas the yield strength is much more sensitive to the initial microstructure.

The predicted dependence of the strengthening effect of niobium on the carbon concentration is shown in Fig. 4.11 . The strength increment plotted on the vertical axis is based on the average effect of niobium in the concentration range 0-1500 parts per million by weight for any given carbon concentrations. The strength increment per weight percent of niobium is obviously very large and this may be reason why niobium is generally not suggested [89].

Fig. 4.12 shows other predictions; although there are no surprises, it is worth noting the error bars. These error bars can be used to identify regions of the input space where further

experiments would be useful. For example, the prediction uncertainties associated with niobium, or with large heat inputs, are much larger than, for instance with changes in the manganese concentration. This is where future experiments could be focussed.

4.5 Application to $2\frac{1}{4}$Cr–1Mo Weld Metals

The $2\frac{1}{4}$Cr1Mo weld metal system is designed primarily for applications where the components will serve at elevated temperatures (450–565 °C) for long periods of time ($\simeq$30 years). This is in contrast to carbon–manganese weld metals which are used in structural applications such as buildings and bridges which are essentially at ambient temperature. Consequently, the post–weld heat treatment is of vital importance to $2\frac{1}{4}$Cr1Mo weld metals, not only to relieve residual stresses but also to generate a stable microstructure in which the carbides hinder creep deformation. The basic values of the variables used in applying the models to $2\frac{1}{4}$Cr1Mo welds are listed in Table 4.4. The specified high–temperature heat treatment is a typical post–weld heat treatment (PWHT).

Input variable	
C (wt%)	0.11
Si (wt%)	0.20
Mn (wt%)	0.80
S (wt%)	0.002
P (wt%)	0.005
Ni (wt%)	0.20
Cr (wt%)	2.25
Mo (wt%)	1.0
V (wt%)	0.0
Cu (wt%)	0.0
Co (wt%)	0.0
W (wt%)	0.0
Ti (wt%)	0.0
O (p.p.m.)	300
B (p.p.m.)	0.0
Nb (p.p.m.)	0.0
Heat input (kJ mm^{-1})	1.5
Interpass temperature (°C)	200
Tempering temperature (°C)	690
Tempering time (h)	8

Table 4.4: The input variables of 2.25Cr–1Mo wt% steel weld metal used in the analysis.

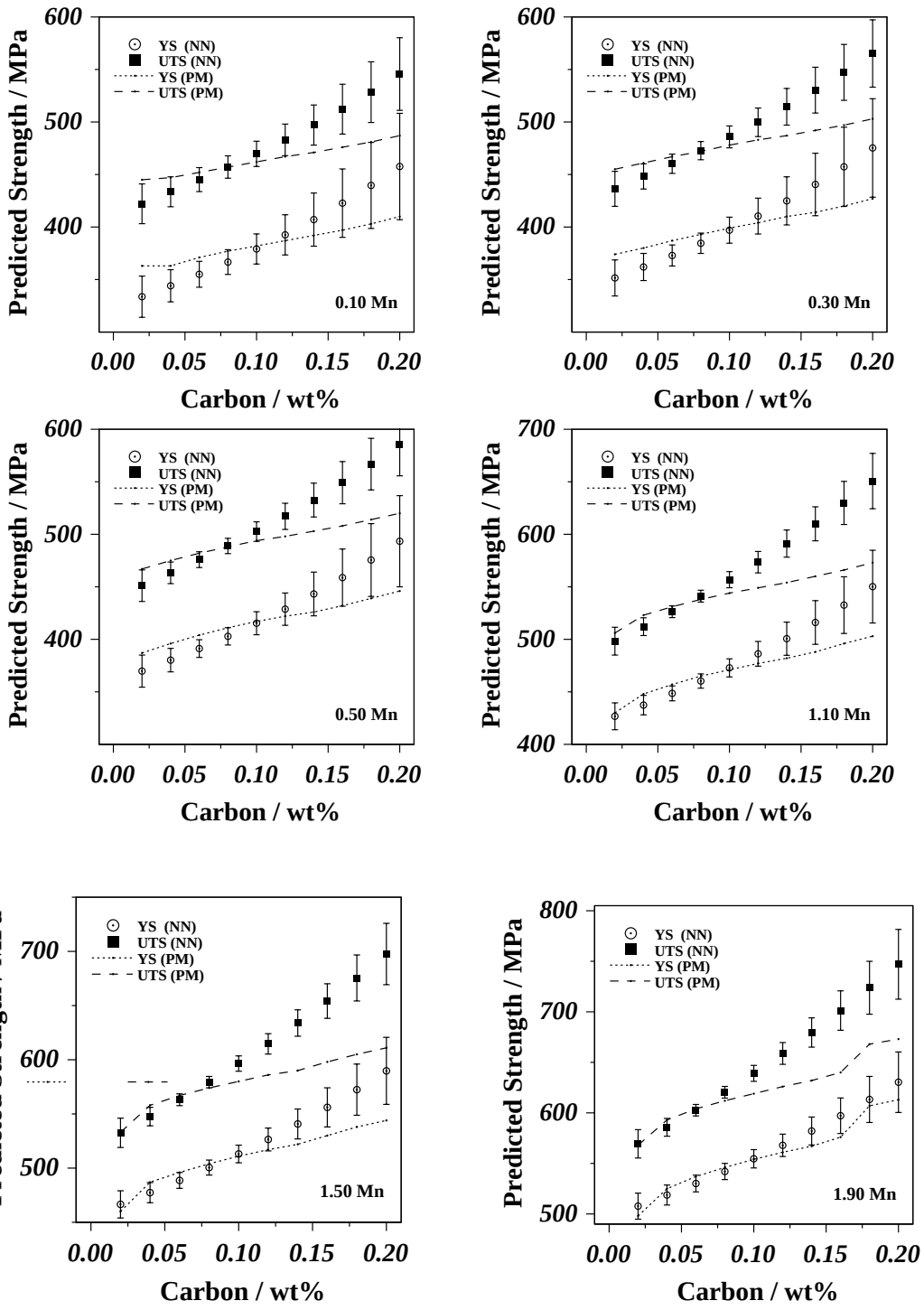

Figure 4.9: A series of calculations for carbon–manganese welds, using both the neural network committee models and an alternative published model [90]

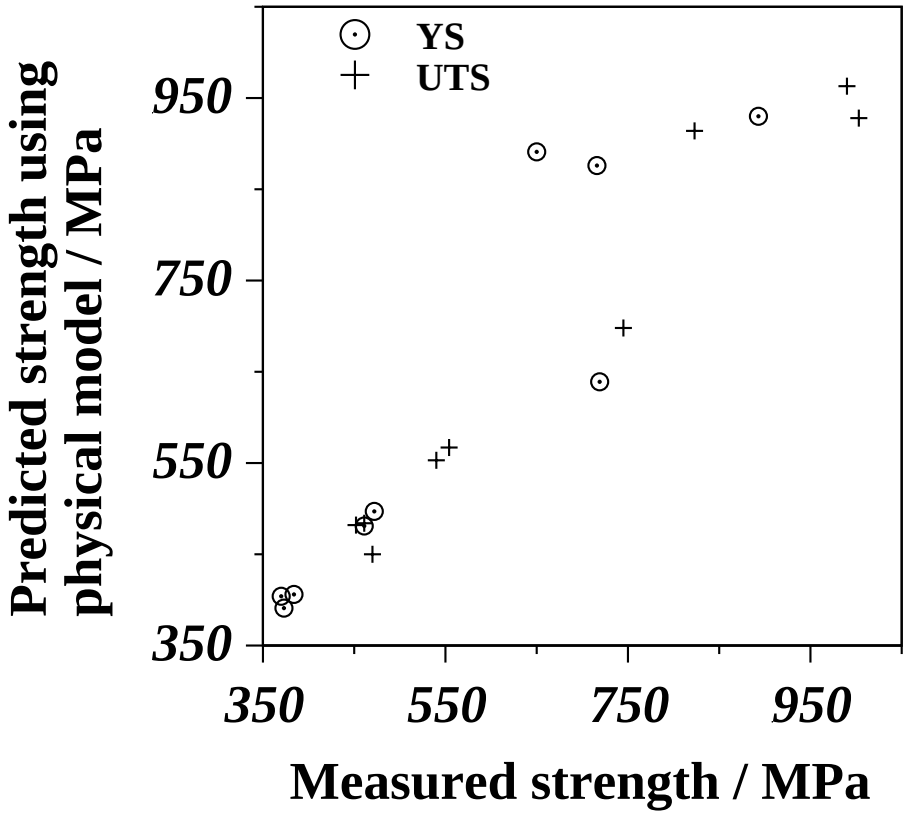

Figure 4.10: Comparison between measured and published physical model calculations [90].

It is notable from the predictions illustrated in Fig. 4.13 that there are greater uncertainties (larger error bars) associated with the estimation of mechanical properties for the $2\frac{1}{4}$Cr1Mo system when compared with the carbon–manganese welds. This is largely because there are fewer data available for $2\frac{1}{4}$Cr1Mo welds.

Another striking feature is that the sensitivity of the strength to alloying elements, in the PWHT condition, is far smaller than in the as–welded condition. This is not surprising given the severe nature of the post–weld heat treatment at 690 °C for 8 hours. It is emphasised that although the yield and tensile strengths are not particularly sensitive to composition in the PWHT condition, this will not be the case for creep properties where the tempering heat treatment is essential for the generation of alloy carbides and to provide a microstructure which has long term stability.

4.6 Conclusions

The yield strength and ultimate tensile strength of ferritic steel weld metal have been analysed using a neural network method within a Bayesian framework. The data used were mostly

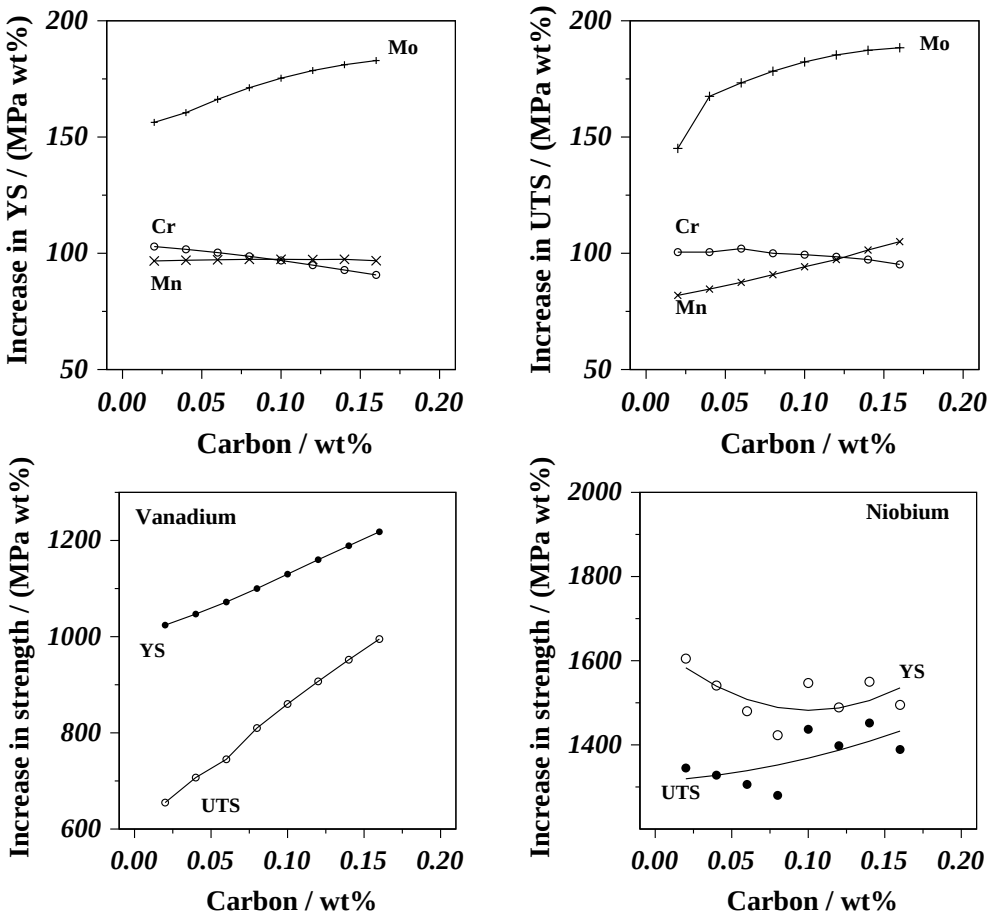

Figure 4.11: Change in strength and the YS/UTS ratio as a function of a wt% of substitutional solute content in carbon–manganese steel welds. The error bars are not included for clarity, but the maximum values are 60.

obtained from the published literature and represent a wide cross–section of alloy compositions and arc–welding processes.

Trends predicted by the models appear to be consistent with those expected metallurgically, although it must be emphasised that only the simplest of trends have been examined since the number of variables involved is very large. The models can be applied widely because the calculation of error bars whose magnitude depends on the local position in the input space is an inherent feature of the neural network used. The error bar is not simply an estimate of the perceived level of noise in the output but also includes an uncertainty associated with fitting the function in the local region of input space. This means that the method is less dangerous in extrapolation or interpolation since it effectively warns when experimental data are lacking or are exceptionally noisy. The work has clearly identified regions of the input space where

further experiments should be encouraged. These models are applied to design new structural, heat resistant and high strength steel welds without any experimental trials are discussed in Chapter 6.

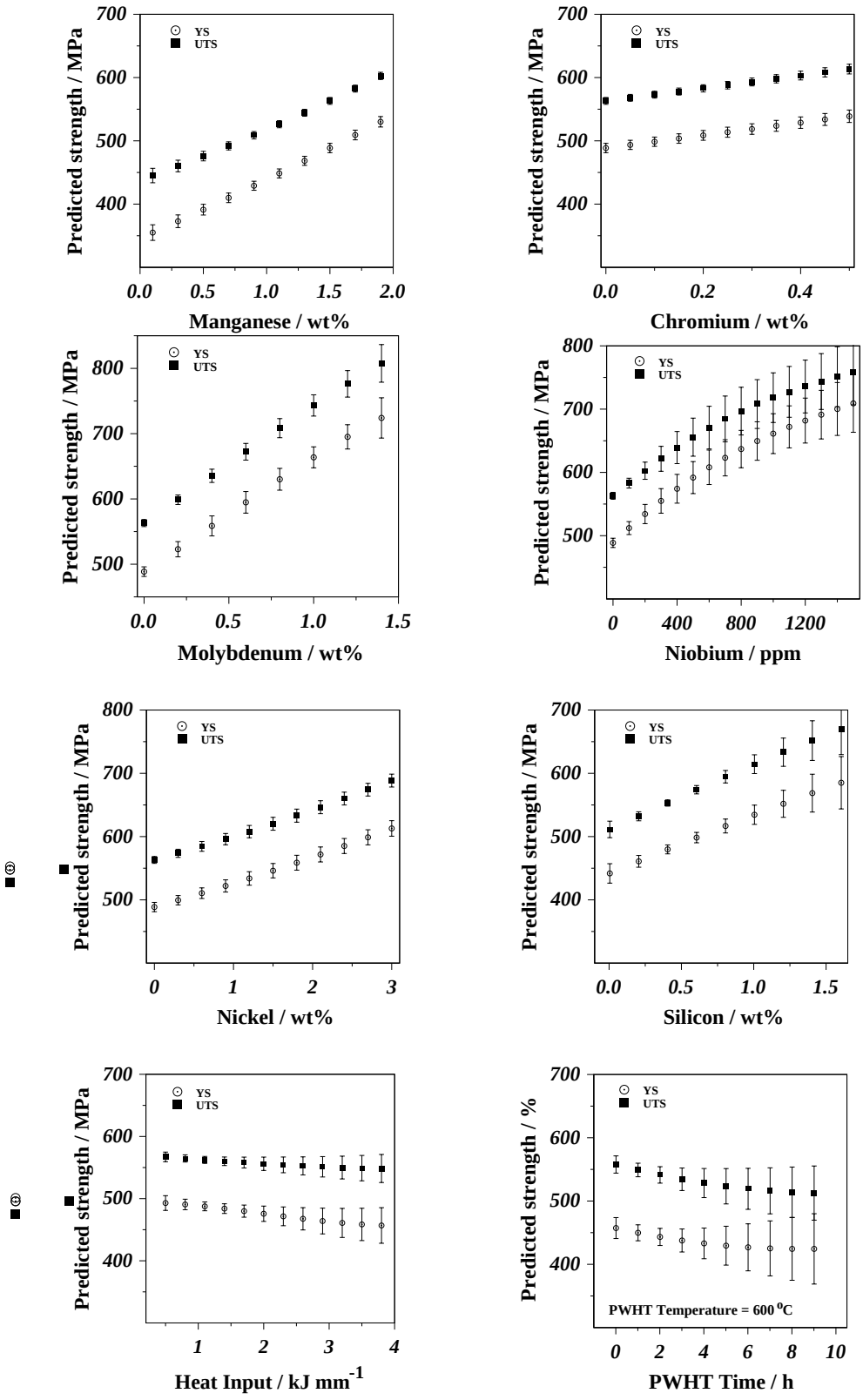

Figure 4.12: Variations in the yield and ultimate tensile strengths of carbon–manganese weld metal as a function of alloying elements and heat treatment.

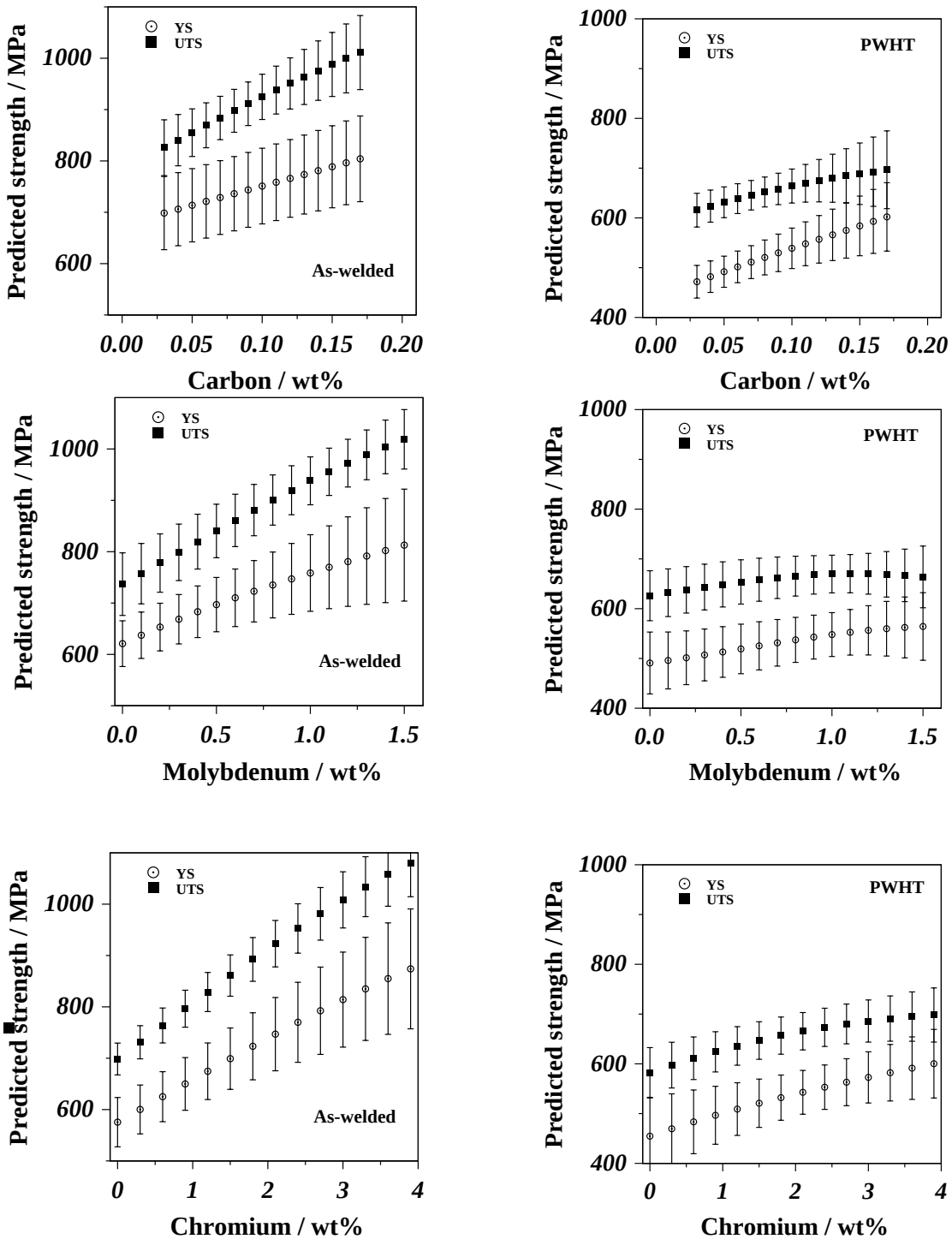

Figure 4.13: The effect of carbon, molybdenum and chromium concentrations on the strength of $2\frac{1}{4}$Cr–1Mo wt% welds in the as–welded and PWHT (690 °C, 8 h) conditions.